A universal RNAi-based logic evaluator that operates in mammalian cells

Keller Rinaudo[1,4], Leonidas Bleris[1,4], Rohan Maddamsetti[1], Sairam Subramanian[2,3], Ron Weiss[2,3] & Yaakov Benenson[1]

Molecular automata[1–3] that combine sensing[4–6], computation[7–12] and actuation[13,14] enable programmable manipulation of biological systems. We use RNA interference (RNAi)[15] in human kidney cells to construct a molecular computing core that implements general Boolean logic[1,3,8–12,16] to make decisions based on endogenous molecular inputs. The state of an endogenous input is encoded by the presence or absence of 'mediator' small interfering RNAs (siRNAs). The encoding rules, combined with a specific arrangement of the siRNA targets in a synthetic gene network[17], allow direct evaluation of any Boolean expression in standard forms using siRNAs and indirect evaluation using endogenous inputs. We demonstrate direct evaluation of expressions with up to five logic variables. Implementation of the encoding rules through sensory up- and down-regulatory links between the inputs and siRNA mediators will allow arbitrary Boolean decision-making using these inputs.

A molecular automaton is an engineered molecular system coupled to a (bio)molecular environment by "flow of incoming messages and the actions of outgoing messages," where the incoming messages are processed by an "intermediate set of elements," that is, a computer[18]. Molecular automata may implement diverse models of computation (digital and analog circuits, state machines, neural networks) to perform a variety of tasks. We suggest a general-purpose design framework for automata that uses logic evaluation to make certain types of decisions based on environmental molecular inputs.

Molecular logic evaluators have been demonstrated *in vitro*[1–3,9,11,12] and in live cells[8,10]. Up until now, only *in vitro* systems[1,12,19] have shown how to evaluate arbitrary logic expressions experimentally, although arbitrary evaluation *in vivo* using transcription factors has been considered theoretically[20,21]. Demonstration that allosteric modulation of small RNAs[22], including ribozymes[1,3,16], riboswitches[4,5] and siRNA[6], regulates gene expression prompted us to suggest that, much like transcription factors, small RNA molecules will enable molecular automata to make *in vivo* evaluations through mediation between endogenous inputs and the downstream molecular 'computing' network.

A logic evaluator operating in an intracellular molecular milieu can serve as a binary decision-making circuit[23], that is, trigger one or two discrete processes in response to inputs from this milieu. The capacity for *in vivo* decision making based on endogenous inputs could find applications in basic research and medicine, such as in the diagnosis of cancer[2,24]. To address this issue, we (i) recast decision-making rules as a logic expression containing intracellular inputs as variables; and (ii) construct a molecular system that produces a molecular output when the expression is evaluated as True for the given input truth values (True when present and False when absent). We propose how to construct such a system for an arbitrary question represented by a logic expression. Although our design suggests separate sensor and evaluator modules, we demonstrate only the evaluator.

There are several theoretically equivalent, but practically different, ways to answer arbitrary logic questions. They generally involve breaking a complex question into a hierarchy of simpler ones. One possibility is to be very stringent with basic modules (e.g., the first input must be True, the second must be False), but connect these modules in a less stringent way where an overall positive result is achieved when any one module gives a positive answer. Another way is to be less stringent within the basic modules (e.g., at least one input has to be in an expected state), but put stringent demands on the combinations of modules, by requiring all answers to be positive simultaneously to give an overall positive answer.

To construct an evaluator that embodies the first approach, we build a biological 'circuit' that comprises two or more mRNA species that encode the same protein, but have different noncoding regions. This protein is the system's output; a biologically active output may function as an actuator. If at least one mRNA species is translated, the resulting output will represent a logic True value, implementing an OR operation[10,12] (**Fig. 1a**). The levels of mRNA species and the output are determined by the presence or absence of the endogenous molecular inputs with the help of molecular mediators. siRNA molecules target untranslated regions and hence are natural candidates for such mediation. First, we fuse different sets of siRNA targets into the 3′-untranslated regions (UTR) of the mRNAs, rendering them susceptible to either of these siRNAs[25]. Next, we establish selective inhibitory links between endogenous inputs and these siRNAs. All inputs must be present at the same time to block all siRNAs and
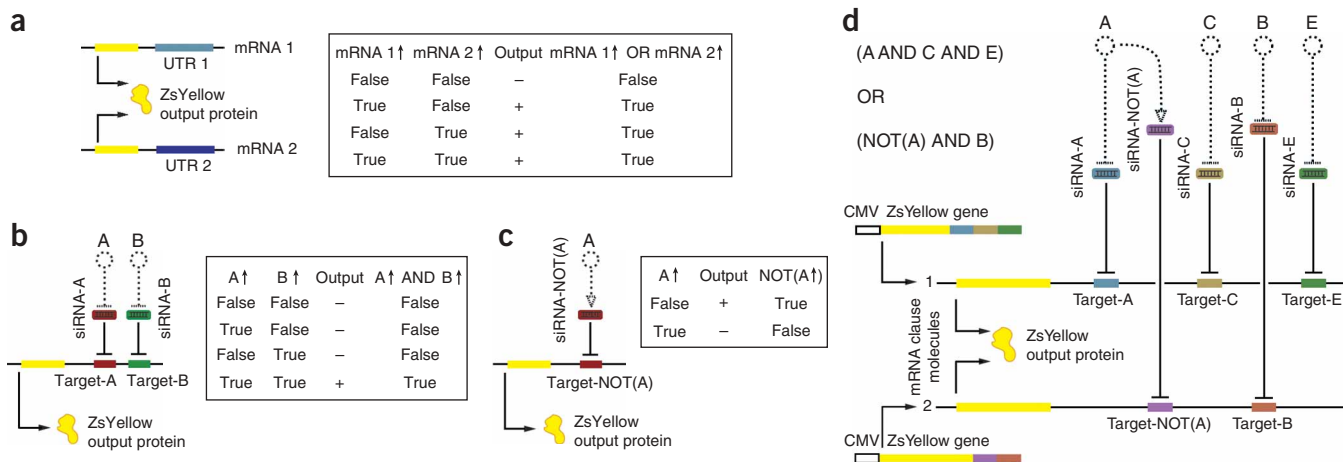
Figure 1 Design of the decision-making automaton that uses a DNF evaluator. (**a**) A circuit that evaluates an OR operation between mRNA molecules. A truth table of an OR operation is shown. An upward arrow indicates the presence of the mRNA. (**b**) A circuit that evaluates an AND operation between the endogenous inputs A and B. Dotted blunt arrows indicate blocking sensory interactions and full blunt arrows indicate downregulation via RNAi. A truth table of the AND operation is shown. Similar circuits are constructed and substituted for each mRNA as in the OR gate in **a**. (**c**) A circuit that evaluates a negation (logic NOT operation) of an endogenous input A and a corresponding truth table. A pointed dotted arrow indicates activating sensory interaction. (**d**) An example of a circuit that, given the sensory links (dotted lines) between the endogenous inputs and the mediator siRNAs, evaluates an indicated DNF expression on these inputs. If, for example, inputs A, B and E are present, the siRNAs that mediate their presence will be inactivated, resulting in a high expression from the clause molecule 1. Even though the siRNA-NOT(A) will be active and will suppress the translation of the output protein ZsYellow from the clause molecule 2, the overall output protein level will qualify as a True result. CMV, human cytomegalovirus immediate-early promoter.

generate output from an mRNA, corresponding to a logic AND operation (**Fig. 1b**). Furthermore, if, for example, inputs A and B block siRNAs that target one mRNA and inputs X and Y block siRNAs that target another, the circuit will generate an output when both A and B are present or when both X and Y are present. This comprises the logic expression (A AND B) OR (X AND Y). If an activating link is established instead, the presence or absence of an input will block or enable output production from the mRNA, respectively. In logical terms, this amounts to a negation of the input 'truth value' (**Fig. 1c**). In the above example, input B activating its mediator siRNA turns the expression into (A AND **NOT**(B)) OR (X AND Y). The same input may block one siRNA and activate another, and thus appear in the expression both as itself and as its negation. This arrangement of input variables and their negations, known as literals, is called a disjunctive normal form (DNF) (**Fig. 1d** and **Supplementary Fig. 1** online). Literals grouped by the AND operation are called 'clauses' and we call the mRNA species modified in their 3′-UTR, as well as the genes that express them, 'clause molecules'.

A biological circuit that enables the second approach comprises mRNA species that produce a transcription factor that represses an output-encoding gene. If the repressor obtained from one mRNA efficiently downregulates the output, all mRNAs must be removed to generate the output, thus implementing an AND logic operation (**Fig. 2a**). As before, we fuse sets of siRNA targets into the 3′-UTR of the repressor mRNAs. However, contrary to the previous case, here endogenous inputs should activate the siRNAs rather than block them. At least one siRNA from each set must be activated to remove all repressor mRNAs and relieve the repression (**Fig. 2b**), corresponding to a logic OR operation (**Fig. 2b**). For example, if inputs A and B activate siRNAs that target one mRNA and inputs X and Y activate siRNAs that target another, we require that at least one of the inputs A and B, and at least one of the inputs X and Y, be present. In logic terms, this constitutes the expression (A OR B) AND (X OR Y). An input that blocks its mediator siRNA is negated in the expression (**Fig. 2c**). This is an example of a conjunctive normal form (CNF)

expression and the circuit is a CNF evaluator (**Fig. 2d**, **Supplementary Fig. 1**). The DNF and CNF standard forms are particularly useful because any logic condition can be evaluated using a corresponding DNF or CNF representation, although one representation may be shorter than the other.

We experimentally implemented DNF and CNF evaluators in immortalized human embryonic kidney cells (293-H). We transfected the cells with the genes comprising the evaluator circuits; we also added, or withheld, mediator siRNA molecules to reflect the anticipated function of the sensory module in accordance with the presence or absence of inputs appearing as variables in expressions (**Fig. 2e**); and we assayed the output levels after 48 h. We chose derivatives of known siRNAs for the current implementation, and constructed five siRNA-target pairs based on published sequences from nonmammalian genes to represent up to five inputs (T1 and T2 from *Renilla reniformis*, FF3 and FF4 from firefly luciferases and SI4 from enhanced green fluorescent protein (eGFP); **Supplementary Table 1** online). We modified the published sequences by sliding them along their parental genes to afford at least a pair of A/U bases on the 5′-end of the molecule and a pair of C/G bases on the 3′-end to ensure asymmetry in RNA-induced silencing complex assembly[26].

Multi-siRNA systems may exhibit undesired crosstalk between individual molecules. We measured this crosstalk, using ZsYellow derivatives with single targets cloned into their 3′-UTR and applying all siRNA molecules at the saturation concentration, one at a time, to each derivative. Crosstalk was negligible for this set of siRNAs (**Supplementary Fig. 2** online), except for a possible minor (~20%) reduction in the ZsYellow level when SI4 siRNA was applied to the FF4 target; this was further reduced to ~10% when the FF4 target was a part of a clause molecule (**Fig. 3**). We then built and tested a number of mRNA clauses for DNF evaluators, fusing the siRNA targets into the 3′-UTR of the ZsYellow output (**Fig. 3**). The results show that complete downregulation is achieved separately by any of the cognate siRNAs but not by the others, as required by the construction (**Fig. 3**). Initially, one of the constructs (ZsYellow-T1-SI4-FF4)
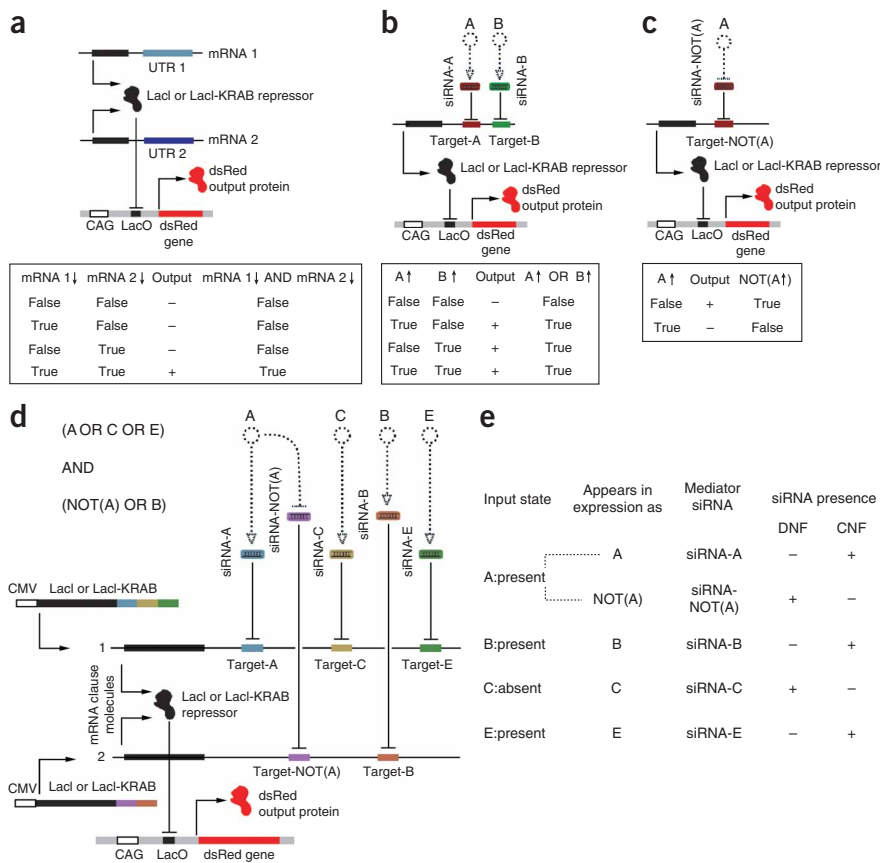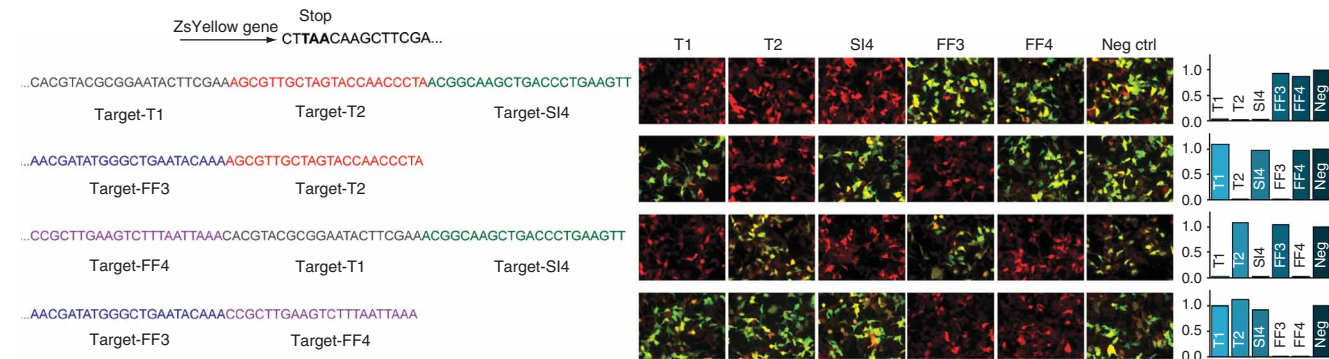
Figure 2 Design of the decision-making automaton that uses a CNF evaluator and automaton's input encoding rules. (**a**) A circuit that evaluates an AND operation between mRNA molecules. A downward arrow in table indicates the absence of the mRNA. CAG, chicken β-actin promoter with CMV enhancer. LacO stands for two adjacent Lac operator sites. KRAB, Krueppel-associated box domain. (**b**) A circuit that evaluates an OR operation between the endogenous inputs A and B. Similar circuits are substituted for all mRNAs from the AND gate. (**c**) A circuit that evaluates a negation (logic NOT) of an endogenous input A. (**d**) A circuit that evaluates the indicated CNF expression. For example, if the inputs B and C are present, siRNA-B and siRNA-C will be activated, downregulating the levels of the LacI repressor translated from the clause molecules 1 and 2. Overall level of the LacI repressor will be low, relieving the suppression from the promoter of the output protein and resulting in a high output level, interpreted as a True evaluation result. (**e**) Rules that link the presence or absence of the endogenous inputs with the presence or absence of their mediator siRNAs, depending on the type of expression (DNF or CNF).

showed incomplete repression by two out of three siRNAs. We performed RNA-folding analysis of the clause sequence with permuted order of targets, and found that an arrangement selected for its low folding energy operates substantially better than the original (**Supplementary Fig. 3** online).

In the next step, we performed evaluation experiments for full DNF and CNF expressions. The connection of the siRNAs and their targets to endogenous input variables is shown in **Supplementary Table 2** online. We constructed circuits to evaluate two expressions in DNF

form, D1: (A AND B AND C) OR (D AND E) and D2: (A AND C AND E) OR (NOT(A) AND B). The same siRNA (FF3) was used differently in D1 and D2, once as a variable E and once as a negated variable NOT(A). As a result, siRNAs T1 and FF3 were never applied together during D2 evaluation. We then tested all possible truth-value assignments for the variables in each expression: 32 for the D1 and 16 for D2 (**Table 1a**). The distribution of output levels in both expressions is shown in **Supplementary Figure 4** online. It demonstrates a clear separation between the groups of False and True outputs as required from a Boolean evaluator, with an average 16-fold difference between output levels in False and True groups. The evaluation of the D1 expression, with all variables being True and no siRNAs present, resulted in more than twice the output of others owing to the parallel

Figure 3 Testing individual DNF clause molecules. The constructs and their common sequence motif that includes a stop codon (top) are shown to the left. We cotransfected 10 pmol of each indicated siRNA (columns) with 100 ng of the indicated clause molecule (rows) and 100 ng of the transfection control plasmid pAmCyan-C1 into 293-H cells and assayed after 48 h. The images combine the fluorescent signal from the AmCyan transfection control (red pseudocolor) and the signal from the ZsYellow protein expressed from the clause molecules (green pseudocolor). Low levels of ZsYellow result in red images whereas coexpression of both proteins results in mostly green and yellow spots. Negative control is a nonsense siRNA provided in the same amount as the active siRNAs. The quantitative results that correspond to the images, obtained by FACS measurements and normalized to the negative control for each construct, are shown on the right.

production of the output from both clause mRNAs. This high value is also interpreted as True[10,12]. In the expression D2, we obtained one imperfect False evaluation (A:T, B:F, C:F, E:T) that generated 0.32 expression units relative to the lowest unsuppressed ('True') output level. This cannot be explained solely by the incomplete downregula-

tion of the clause molecule Target-(E)-(A)-(C) by SI4, as the same siRNA worked about two to three times more efficiently when the clause molecule was tested alone (e.g., see **Supplementary Fig. 3** online). However, increasing the amount of the SI4 siRNA from 2.5 pmol to 10 pmol per transfection resulted in a repression

Table 1 Operation of the Boolean evaluator

a

D1: (A AND B AND C) OR (D AND E)

A B C D E	siRNA A B C D E	D1	Int. a.u.	A B C D E	siRNA A B C D E	D1	Int. a.u.
F F F F F	+ + + + +	F	0.03	T F F F F	– + + + +	F	0.02
F F F F T	+ + + + –	F	0.02	T F F F T	– + + + –	F	0.03
F F F T F	+ + + – +	F	0.03	T F F T F	– + + – +	F	0.03
F F F T T	+ + + – –	T	1.23	T F F T T	– + + – –	T	1.23
F F T F F	+ + – + +	F	0.03	T F T F F	– + – + +	F	0.02
F F T F T	+ + – + –	F	0.03	T F T F T	– + – + –	F	0.04
F F T T F	+ + – – +	F	0.03	T F T T F	– + – – +	F	0.03
F F T T T	+ + – – –	T	1.19	T F T T T	– + – – –	T	1.25
F T F F F	+ – + + +	F	0.04	T T F F F	– – + + +	F	0.07
F T F F T	+ – + + –	F	0.05	T T F F T	– – + + –	F	0.09
F T F T F	+ – + – +	F	0.03	T T F T F	– – + – +	F	0.05
F T F T T	+ – + – –	T	1.01	T T F T T	– – + – –	T	1.24
F T T F F	+ – – + +	F	0.14	T T T F F	– – – + +	F	1.00
F T T F T	+ – – + –	F	0.18	T T T F T	– – – + –	T	1.02
F T T T F	+ – – – +	F	0.09	T T T T F	– – – – +	T	1.02
F T T T T	+ – – – –	T	1.10	T T T T T	– – – – –	T	2.98

D2: (A AND C AND E) OR (B AND NOT(A))

A B C E	siRNA A B C E NOT(A)	D2	Int. a.u.
F F F F	+ + + + –	F	0.03
F F F T	+ + + – –	F	0.12
F F T F	+ + – + –	F	0.03
F F T T	+ + – – –	F	0.22
F T F F	+ – + + –	T	1.00
F T F T	+ – + – –	T	1.11
F T T F	+ – – + –	T	1.01
F T T T	+ – – – –	T	1.28
T F F F	– + + + +	F	0.03
T F F T	– + + – +	F	0.32
T F T F	– + – + +	F	0.03
T F T T	– + – – +	T	1.20
T T F F	– – + + +	F	0.03
T T F T	– – + – +	F	0.18
T T T F	– – – + +	F	0.02
T T T T	– – – – +	T	1.02

b

C1: (D OR E)

D E	siRNA D E	C1	LacI + single targets Neg Ctrl 10	20	Int. a.u.	LacI-KRAB + triple targets Neg Ctrl 5	10	Int. a.u.
F F	– –	F			0.30			0.15
F T	– +	T			1.25			1.02
T F	+ –	T			1.00			1.00
T T	+ +	T			1.23			1.35

C2: (D) AND (E)

D E	C2	LacI + triple targets Neg Ctrl 5	10	Int. a.u.
F F	F			0.12
F T	F			0.31
T F	F			0.31
T T	T			1.00

c

E1: (D)

D	siRNA-D	E1	NOT(E1)	Int., a.u. zsYellow	dsRed
F	+	F	T	<0.01	1.00
T	–	T	F	1.00	0.23

(**a**) Two expressions in DNF form are evaluated for all possible variable assignments as indicated in the figure. 2.5 pmol of each input siRNA (or 2.5 pmol of the negative control siRNA in the case of an absent input siRNA) were cotransfected with 100 ng of each clause molecule and 100 ng of the pAmCyan-C1 transfection control into 293-H cells and assayed after 48 h. The quantitative results corresponding to the images that were obtained using FACS are shown on the right (see Methods). Red pseudocolor represents the transfection control protein AmCyan and the green color represents the output protein ZsYellow. (**b**) An evaluation of two CNF expressions. In C1 evaluation experiments using LacI, 10 pmol of each siRNA, 50 ng of the CMV-LacI-FF3-FF4 clause molecule, 200 ng of CAGOP-dsRed-monomer reporter and 100 ng of pAmCyan-C1 transfection control were cotransfected into 293-H cells and assayed after 48 h. The expression levels of the reporter obtained by FACS are given relative to the control experiments where active siRNA was replaced with the same level of nonsense siRNA (first row of images). In C1 evaluation experiments using LacI-KRAB, 5 pmol of each siRNA, 5 ng of the CMV-LacI-KRAB-FF3x3-FF4x3 clause molecule, 200 ng of CAGOP-dsRed-monomer reporter and 100 ng of pAmCyan-C1 transfection control were cotransfected into 293-H cells and imaged after 48 h. The expression levels of the reporter given in the figure were obtained by FACS using 100 ng of pZsYellow-C1 transfection control instead of pAmCyan-C1 and they are given relative to the control experiments where active siRNA was replaced with the same level of nonsense siRNA (first row of images). In C2 evaluation experiments, 5 pmol of each siRNA, 50 ng of CMV-LacI-FF3x3 and CMV-LacI-FF4x3 clause molecules, 200 ng of CAGOP-dsRed-monomer reporter and 100 ng of pAmCyan-C1 transfection control plasmids were cotransfected into 293-H cells and assayed after 48 h. It was quantified similarly to the C1 experiments with LacI. Blue pseudocolor represents the transfection control protein AmCyan and the red color represents the reporter protein dsRed-monomer. (**c**) A demonstration of anticorrelated evaluation results provided by two circuits operating in parallel. 10 pmol of siRNA (or nonsense siRNA), 100 ng of pZsYellow-F3x3 and 50 ng of CMV-LacI-F3x3 clause molecules and 200 ng of CAGOP-dsRed-monomer reporter were cotransfected into 293-H cells and assayed after 48 h. Each reporter (ZsYellow and dsRed) was quantified independently and given relative to their respective True expression levels.

improvement down to 0.08 units (data not shown). Similar improvement was obtained with the (A:F, B:F, C:T, E:T) evaluation that generates 0.22 units under standard conditions but may be reduced ∼fourfold by an increase in the T1 siRNA level.

We next fused siRNA targets to the 3′-UTR of the LacI repressor[27] driven by the cytomegalovirus (CMV) promoter (**Fig. 1d**) to evaluate a single-clause CNF expression C1: (D OR E) and a two-clause, two-variable expression C2: (D) AND (E). In the latter expression, each single-variable clause molecule was modified by the triple tandem repeat of the target instead of a single occurrence to improve repression efficiency[28]. The dsRed-monomer reporter of the truth values in CNF evaluators was under the control of the CAGOP promoter[27] (**Fig. 2d**). The CNF evaluator (**Table 1b**) performs an AND operation between clauses and an OR operation within a clause; however, currently the CNF evaluator is quantitatively less robust than its DNF counterpart. We expect that tight repression on the one hand, and efficient down-regulation by the siRNA on the other, will improve its performance. Apart from increasing the strength of the operator (CAGOP versus CMV-LacO) and fusing tandem repeats, we also tested a stronger repressor LacI-KRAB and thus were able to double the performance of the C1 evaluator (**Table 1b**). Nonetheless, additional fine-tuning of both the operator and the targets is still needed to improve scalability.

Our design framework allows parallel evaluation of an expression and its negation; this can improve the overall performance of the system. When two anticorrelated outputs are produced in parallel, their difference is a better indicator of the process outcome than individual outputs[2]. For example, a DNF expression *e* generates an evaluator circuit and a sensory interface that correspond to this expression; the result is judged by output O1. We can construct a parallel circuit where the output O1 is replaced by a repressor that regulates an expression of a different output O2. It is easy to see that when both circuits use the same sensory interface, the output O2 reflects the truth value of the expression NOT(*e*) and therefore the outputs O1 and O2 are anticorrelated. **Table 1c** demonstrates this feature for the trivial single-literal expression E1: (D).

This report represents a step toward *in vivo* programmable decision-making molecular automata by implementation of a computing core that evaluates logic expressions in standard forms. These forms, evaluated using two-level logic circuits, may entail an exponential increase in size for representing certain logic functions relative to multilevel circuits[12]. However, a reduction in the number of computation stages reduces the overall processing time of the circuit. Noise and signal degradation are an issue in both circuit architectures; signal restoration, that is, improving the ON/OFF ratio at intermediate stages greatly improves scalability and performance. In the case where the two-level logic representation cannot be implemented efficiently owing to the accumulation of incompletely repressed clauses, it is also possible to subdivide the computation into a hierarchy and introduce signal restoration. Currently the performance of our circuits is comparable to similar *in vitro* and *in vivo* logic networks that do not use this restoration. Certain mammalian transcriptional logic gates achieve a ∼20-fold average difference between the molecular levels that correspond to True and False outputs in 2–3 input logic gates[10], and an evolutionarily optimized single-input cascade[29] enables about a sevenfold difference between these outputs. *In vitro* and *in vivo* riboswitch systems[1,4,5,13,16] and a *Fok*I-based protein-release system[14] achieve ∼10- to 100-fold True to False ratios. Large-scale *in vitro* systems[1–3] show ≤10-fold True:False ratio. An order-of-magnitude difference in our experiments may be enough for many applications. However, we expect that signal-restoration motifs will improve performance, as suggested by

a >1,000-fold On:Off ratio in a transcriptional circuit[30] and a >100-fold True:False ratio in an *in vitro* system[12].

We propose a sensory mechanism whereby one siRNA mediates the presence, and another the absence, of a given input through direct and opposite regulatory links, with the latter implementing the logic NOT operation[12] (**Supplementary Fig. 5** online). We envision both activation and inactivation mechanisms of siRNA-like molecules by diverse molecular inputs, as required by the automaton architecture. For example, recent work[6] has demonstrated both inhibition and activation of siRNA by a small molecule whereas a DNA automaton[2] used distinct subsequences of an mRNA molecule to oppositely regulate two different siRNA-like double-stranded DNA structures. An alternative mechanism would involve only one kind of regulatory link between the input and one of the mediators, with an additional inhibitory interaction between this and the complementary mediator (**Supplementary Fig. 5**). Our approach seems preferable for two reasons. First, in our arrangement, we require two molecular interactions for an input that is tested for either presence or absence, and four interactions when an input is tested for both (that is, appears both as a positive and a negative literal in a logic expression). In the alternative, an input tested for its absence requires three interactions (**Supplementary Fig. 5**), increasing the total number of interactions per circuit. Second, our design requires at most two consecutive interactions upstream of the computing core, whereas the alternative requires three when we test for an input absence; an increased number of steps will increase the probability of a failure.

Implementation of our circuits is challenging as it requires multiple and efficient siRNA structures with minimal crosstalk. We have largely overcome these challenges by using siRNA molecules developed with the help of computer-aided design[15]. In the future, the utility of such design principles for the construction of automata could be further improved by taking into account the selectivity and efficiency of siRNA-mediators both as sensors and as regulators of gene expression. Ultimately, molecular computing and synthetic biology may create molecular information-processing networks that are better than natural ones in their quantitative performance while permitting novel functionalities.

METHODS

siRNA molecules. The sequences of the ribo-oligonucleotides are given in **Supplementary Table 1**. T1 and T2 siRNAs were annealed from gel-purified oligomers (Proligo); gel-purified SI4 siRNA (Proligo) was used as provided by the manufacturers. FF3 and FF4 siRNAs were annealed from desalted oligomers (Dharmacon) after purification from 20% denaturing PAGE. To anneal RNA oligomers, equimolar amounts (50 or 200 μM) of the sense and antisense oligomers were mixed in 50 mM NaCl, 10 mM Tris-HCl pH 8.0, 1 mM EDTA and 0.5 U/μl Superase-In (Ambion), heated to 95 °C and slowly cooled down to 10 °C in a PCR block for 50 min. The size and purity of the siRNAs were verified using 3.5% Metaphor agarose gel (Cambrex).

Recombinant DNA constructs. Single- and multiple-target clause molecules used in DNF evaluators were derived from the pZsYellow-C1 vector (Clontech) digested with *Bam*HI and *Xho*I (New England Biolabs) and purified from agarose gel using a Gel Purification Kit (Qiagene). The deoxyribonucleotides (Sigma, **Supplementary Table 1**), comprising the DNA inserts into 3′-UTR of ZsYellow gene, were designed with a stop codon 10 bp upstream of the siRNA target sites and ready-to-ligate sticky ends. They were obtained either gel purified and phosphorylated (T1, T2 and SI4 inserts) or desalted (FF3, FF4, FF3x3, FF4x3, T1.T2.SI4, FF3.FF4, FF4.T1.SI4 and FF3.T2 inserts). The latter oligomers were gel purified in-house using 8% or 12% PAGE. Oligonucleotides at 25 or 12.5 μM were annealed in TE buffer (10 mM Tris-HCl and 1 mM EDTA, pH 8.0) supplemented with 50 mM NaCl in a PCR machine block by heating to 95 °C and cooling down to 10 °C for 50 min.

When required, double-stranded inserts at 3 μM were phosphorylated in 50 μl Polynucleotide Kinase (PNK) reaction buffer (New England Biolabs) by 15 units of PNK and 1 mM ATP (Invitrogen) for 30 min at 37 °C before subcloning (see standard subcloning protocol 1, **Supplementary Methods**).

LacI-derived CNF clause molecule CMV-LacI-FF3-FF4 was constructed by replacing the ZsYellow gene with LacI gene in the DNF clause molecule pZsYellow-FF3-FF4. The gene encoding LacI was amplified from the pCMV-LacI plasmid (LacSwitch II Inducible Mammalian Expression System kit, Stratagene) using the primers 5′-CCAGCTAGCGAGGTACCCTCCCACCATG-3′ and 5′-CCAAGATCTTCAAACCTTCCTCTTCTTCTTAGG-3′ with engineered BglII and NheI restriction sites. The PCR product was digested with BglII and NheI enzymes and subcloned into the backbone vector after the ZsYellow gene was excised with BglII and NheI enzymes (see standard subcloning protocol 1, **Supplementary Methods**).

The colonies were verified by colony PCR using the following primers: 5′-CGTCAATGGGAGTTTGTTTTG-3′ and 5′-GCGCCGAGACAGAACTTAAT-3′, and further by sequencing the LacI and the 3′-UTR insert regions. LacI-derived CNF clause molecules CMV-LacI-F3x3 and CMV-LacI-F4x3 were obtained by removing the T2 target site from the CMV-LacI-T2 plasmid (constructed similarly to the CMV-LacI-FF3-FF4 described above) with BamHI and XhoI enzymes and replacing it with the inserts F3x3 and F4x3.

Construction of the reporter plasmid pCAGOP-DsRed-Monomer-N1 was done as follows. The CMV promoter in pDsRed-Monomer-N1 (Clontech) was replaced by a human EF1-α promoter flanked by PacI and EcoRI sites to construct pHef1α-DsRed-Monomer-N1. The EF1-α promoter was amplified by PCR from pLEIGW. The CAGOP promoter was PCR-amplified using primers 5′-ACTAGGTTAATTAATAGT TATTAATAGTAATCAATTACGG-3′ and 5′-GAT GAAGAATTCAGGCCGAGGCGGCCGTCGACGTTAACGCTAGCGGCCGTA ATGGCCTACCTGTGGGAGTAACGCGGTCAG-3′. The PCR product and pHef1α-DsRed-Monomer-N1 were digested with PacI and EcoRI and ligated to construct pCAGOP-DsRed-monomer-N1 (see standard subcloning protocol 2, **Supplementary Methods**).

CMV-LacI-KRAB-F3x3-F4x4: pCMV-LacI-KRAB was constructed from plasmid pCMV-LacI (Stratagene) and pLV-tTRKRAB-Red, which contains the KRAB repression domain. A PCR of pCMV-LacI was done using primers 5′-ACTAAGCACCTGCACTCCAGGAACGCACGGGTGTTGGGTCGTTTG-3′ and 5′-CTAGATCACCTGCATCACTGCCCGCTTTCCAGTCGGGAAACCTG-3′ to eliminate the stop codon of the gene encoding LacI and introduce AarI sites. A PCR of pLV-tTRKRAB-Red was done using primers 5′-CTAATCC ACCTGCACTCGCAGCCAAAAAAGAAGAGAAAGGTCGAC-3′ and 5′-ATCA TCCACCTGCATCACCTGTTAAACTGATGATTTGATTTCAAATGC-3′ to amplify a fragment containing the KRAB domain flanked by AarI sites. Digestion of the PCR fragments using AarI and subsequent ligation resulted in the cloning of pCMV-LacI-KRAB with the KRAB repression domain fused in frame at the C-terminal of LacI. The LacI-KRAB fragment was PCR amplified using primers 5′-ACTACTGCTAGCTCCCACCATGAAACCAGTAACG-3′ and 5′-CATCATAGATCTTTAAACTGATGATTTGATTTCAAATG-3′. The PCR product was subcloned instead of the ZsYellow into pZsYellow-FF3-FF4 using the BglII and NheI sites to create pCMV-LacI-KRAB-FF3-FF4 (see standard subcloning protocol 2, **Supplementary Methods**).

The insert F3x3-F4x3 was constructed by ligating (ligation protocol, **Supplementary Methods**) annealed and appropriately phosphorylated fragments F34x3.I and F34x3.II (**Supplementary Table 1**). The ligated insert was gel purified from 3.0% Metaphor agarose gel using a gel purification kit, phosphorylated and subcloned into pCMV-LacI-KRAB-FF3-FF4 after excision of the FF3-FF4 insert with BamHI and XhoI enzymes to afford CMV-LacI-KRAB-F3x3-F4x4 construct.

Cell culture. Serum-free media (SFM) adapted 293-H cells (Invitrogen) were used throughout the experiments. The cells were grown at 37 °C, 100% humidity and 5% CO$_2$. The cells were initially transferred into CD-293 medium and a week later moved to the Dulbecco's modified Eagle's medium (DMEM, Invitrogen) supplemented with 0.1 mM of MEM nonessential amino acids (Invitrogen), 0.045 units/ml of penicillin and 0.045 μg/ml streptomycin (penicillin-streptomycin liquid, Invitrogen), and 10% FBS (Invitrogen). The adherent culture was maintained indefinitely in this medium by trypsinizing

with trypsin-EDTA (0.25% trypsin with EDTA·Na$_4$, Invitrogen) and diluting in a fresh medium upon reaching 50–90% confluence.

For transfection experiments, ∼90–120 thousand cells in 1 ml of complete medium were plated into each well of 12-well uncoated glass-bottom (MatTek) or plastic (Falcon) plates and grown for ∼24 h. Shortly before transfection, the medium was replaced with 1 ml DMEM without supplements with a single medium wash step. Transfection mixtures were prepared by mixing all nucleic acids, including the plasmids and the siRNAs into 40 μl of DMEM. 2.4 μl of the Plus reagent (Invitrogen) was added to the final mix and incubated for 20 min at 24 °C. In parallel, 1.6 μl lipofectamine (Invitrogen) were mixed with 40 μl DMEM. Plus- and lipofectamine-containing solutions were mixed and incubated for 20 more min at 24 ºC before application to the cells. The transfection mixture (typically 90 μl) was applied to the wells and mixed with the medium by gentle shaking. Three hours after transfection, 120 μl FBS was added to the wells and the cells were incubated for up to 48 h before the analysis.

The cells were prepared for the fluorescent-activated cell sorting (FACS) analysis by trypsinizing each well with 0.5 ml 0.25% trypsin-EDTA, collecting the cell suspension and centrifuging at 2,655 gs for 2 min. Trypsin was removed and the pellet resuspended by short vortexing in 0.5 ml PBS buffer (Invitrogen).

Microscope measurements and image processing. All microscope images were taken from live cells grown in glass-bottom wells in the transfection medium supplemented with 10% FBS. We used the Zeiss Axiovert 200 microscope equipped with Sutter filter wheels, Prior mechanized stage and an environmental chamber (Solent) held at 37 °C during measurements. The images were collected by an Orca ERII camera cooled to –60 °C, in the high precision (14 bit) mode using a 20× PlanApochromat NA 0.8, PH2 objective. The collection setting for the fluorophores in crosstalk measurements and DNF evaluation experiments were S500/20x (excitation) and S535/30m (emission) filters for ZsYellow; and S430/25x (excitation) and S470/30m (emission) for AmCyan. A dichroic mirror 86004v2bs (Chroma) was used for both fluorophores. In CNF evaluation experiments the settings were: S565/55x (excitation) and S650/75m (emission) filters with a dichroic mirror 86021bs (Chroma) for dsRed-monomer, and AmCyan settings as above. For the anticorrelated output experiment we used yellow fluorescent setting as above and S565/25x (excitation) and S650/75m (emission) filters with a dichroic mirror 86007bs (Chroma) for dsRed-monomer. Data collection and processing were performed by the Metamorph 7.0 software (Molecular Devices). After background subtraction, the relative intensities of the internal transfection control and the reporter protein were adjusted to equalize the apparent intensity of both in the negative control experiments. The settings were applied uniformly to all images taken from the crosstalk experiments and DNF evaluations. A different setting was applied to the images taken from the CNF evaluation experiments and to the anticorrelated output experiments because the constructs had a different baseline fluorescence.

FACS measurements and data analysis. In crosstalk measurements and DNF evaluation experiments the cells were analyzed on a BD LSRII flow analyzer. ZsYellow was measured using a 488 nm laser and a 530/30 emission filter. AmCyan was measured with a 405 nm laser and a 450/50 emission filter. The data were analyzed using FlowJo software (FlowJo LLC). For each sample, the normalized ZsYellow level was calculated by dividing the compensated mean ZsYellow intensity in AmCyan-positive cells (obtained by putting the threshold at the highest autofluorescence value of AmCyan-negative cells) by the compensated mean AmCyan value in these cells. The normalized values collected in a single experiment were further divided by the ZsYellow/AmCyan ratio in the negative control samples. In the DNF evaluation experiments, the ratios were normalized to the lowest value in the unrepressed group of experiments. The same analyzer was used for the CNF evaluation experiments with LacI repressor. AmCyan was measured with a 405 nm laser and a 525/50 emission filter and dsRed-monomer with a 488 nm laser and a 575/26 emission filter. For each sample, the normalized dsRed level was calculated by dividing the compensated mean dsRed intensity (corrected for the cell autofluorescence) in AmCyan positive cells by the compensated and corrected mean AmCyan values in these cells. These values were divided by similarly calculated values in the negative controls where nonsense siRNA was applied at the same concentration as in the experiments. A MoFlo cell sorter (Darko) was used to analyze

the C1 evaluation with LacI-KRAB repressor and the anticorrelated output experiments. ZsYellow was measured with a 488 nm laser and a 530/40 emission filter and dsRed monomer with a 568 nm laser and a 630/30 emission filter. The data from C1 evaluation were processed similarly to those described above. In the anticorrelated output experiment, for each reporter the mean value of its intensity in the transfected cells was weighted by the relative number of transfected cells and these numbers were independently factored for each reporter to the higher of the two values. All reported values (except for the data in **Supplementary Fig. 3**) are averages of two independent experiments, and at least 30,000 qualified events were collected for each sample.

1. Stojanovic, M.N. & Stefanovic, D. A deoxyribozyme-based molecular automaton. *Nat. Biotechnol.* **21**, 1069–1074 (2003).
2. Benenson, Y., Gil, B., Ben-Dor, U., Adar, R. & Shapiro, E. An autonomous molecular computer for logical control of gene expression. *Nature* **429**, 423–429 (2004).
3. Macdonald, J. *et al.* Medium scale integration of molecular logic gates in an automaton. *Nano Lett.* **6**, 2598–2603 (2006).
4. Isaacs, F.J. *et al.* Engineered riboregulators enable post-transcriptional control of gene expression. *Nat. Biotechnol.* **22**, 841–847 (2004).
5. Bayer, T.S. & Smolke, C.D. Programmable ligand-controlled riboregulators of eukaryotic gene expression. *Nat. Biotechnol.* **23**, 337–343 (2005).
6. An, C.I., Trinh, V.B. & Yokobayashi, Y. Artificial control of gene expression in mammalian cells by modulating RNA interference through aptamer-small molecule interaction. *RNA* **12**, 710–716 (2006).
7. Ezziane, Z. DNA computing: applications and challenges. *Nanotechnology* **17**, R27–R39 (2006).
8. Basu, S. & Weiss, R. The device physics of cellular logic gates. *First Workshop on Non-Silicon Computation* Boston, February 3 2002 <http://www.cs.cmu.edu/~phoenix/nsc1/paper/3-2.pdf> 54–61.
9. Balzani, V., Credi, A. & Venturi, M. Molecular logic circuits. *ChemPhysChem* **4**, 49–59 (2003).
10. Kramer, B.P., Fischer, C. & Fussenegger, M. BioLogic gates enable logical transcription control in mammalian cells. *Biotechnol. Bioeng.* **87**, 478–484 (2004).
11. Baron, R., Lioubashevski, O., Katz, E., Niazov, T. & Willner, I. Elementary arithmetic operations by enzymes: A model for metabolic pathway based computing. *Angew. Chem. Int. Ed.* **45**, 1572–1576 (2006).
12. Seelig, G., Soloveichik, D., Zhang, D.Y. & Winfree, E. Enzyme-free nucleic acid logic circuits. *Science* **314**, 1585–1588 (2006).
13. Kolpashchikov, D.M. & Stojanovic, M.N. Boolean control of aptamer binding sites. *J. Am. Chem. Soc.* **127**, 11348–11351 (2005).
14. Beyer, S. & Simmel, F.C. A modular DNA signal translator for the controlled release of a protein by an aptamer. *Nucleic Acids Res.* **34**, 1581–1587 (2006).
15. Eckstein, F. Small non-coding RNAs as magic bullets. *Trends Biochem. Sci.* **30**, 445–452 (2005).
16. Penchovsky, R. & Breaker, R.R. Computational design and experimental validation of oligonucleotide-sensing allosteric ribozymes. *Nat. Biotechnol.* **23**, 1424–1433 (2005).
17. Hasty, J., McMillen, D. & Collins, J.J. Engineered gene circuits. *Nature* **420**, 224–230 (2002).
18. Wiener, N. *Cybernetics* (MIT Press, New York, 1948).
19. Soloveichik, D. & Winfree, E. The computational power of Benenson automata. *Theor. Comp. Sci.* **244**, 279–297 (2005).
20. Weiss, R., Homsy, G. & Knight, T.F. Toward *in vivo* digital circuits. in *Natural Computing Series* (eds. Winfree, E. Landweber, L.F.) 275–295, (Springer, Heidelberg, 2002).
21. Buchler, N.E., Gerland, U. & Hwa, T. On schemes of combinatorial transcription logic. *Proc. Natl. Acad. Sci. USA* **100**, 5136–5141 (2003).
22. Isaacs, F.J., Dwyer, D.J. & Collins, J.J. RNA synthetic biology. *Nat. Biotechnol.* **24**, 545–554 (2006).
23. Laslo, P. *et al.* Multilineage transcriptional priming and determination of alternate hematopoietic cell fates. *Cell* **126**, 755–766 (2006).
24. Rosenwald, A. *et al.* Relation of gene expression phenotype to immunoglobulin mutation genotype in B cell chronic lymphocytic leukemia. *J. Exp. Med.* **194**, 1639–1647 (2001).
25. Doench, J.G. & Sharp, P.A. Specificity of microRNA target selection in translational repression. *Genes Dev.* **18**, 504–511 (2004).
26. Schwarz, D.S. *et al.* Asymmetry in the assembly of the RNAi enzyme complex. *Cell* **115**, 199–208 (2003).
27. Caron, L. *et al.* The Lac repressor provides a reversible gene expression system in undifferentiated and differentiated embryonic stem cell. *Cell. Mol. Life Sci.* **62**, 1605–1612 (2005).
28. Sullivan, C.S. & Ganem, D. A virus-encoded inhibitor that blocks RNA interference in mammalian cells. *J. Virol.* **79**, 7371–7379 (2005).
29. Yokobayashi, Y., Weiss, R. & Arnold, F.H. Directed evolution of a genetic circuit. *Proc. Natl. Acad. Sci. USA* **99**, 16587–16591 (2002).
30. Hooshangi, S., Thiberge, S. & Weiss, R. Ultrasensitivity and noise propagation in a synthetic transcriptional cascade. *Proc. Natl. Acad. Sci. USA* **102**, 3581–3586 (2005).